

Diplomarbeit

**A RETROSPECTIVE ANALYSIS OF SINGLE
ROTATION CTA OF THE NECK IN CEREBRAL
WHOLE BRAIN CT-PERFUSION – EVALUATION OF
A ONE-STOP-IMAGING CT STROKE PROTOCOL**

eingereicht von

Siong Chuong WONG

zur Erlangung des akademischen Grades

Doktor(in) der gesamten Heilkunde

(Dr. med. univ.)

an der

Medizinischen Universität Graz

ausgeführt am

Institut für Diagnostische und Interventionelle Radiologie,

Klinikum Klagenfurt am Wörthersee

unter der Anleitung von

Univ.-Prof. Dr. Klaus Hausegger

Univ.-Prof. Dr. Hannes Deutschmann

Graz, 25.10.2019

Eidesstattliche Erklärung

Ich erkläre ehrenwörtlich, dass ich die vorliegende Arbeit selbstständig und ohne fremde Hilfe verfasst habe, andere als die angegebenen Quellen nicht verwendet habe und die den benutzten Quellen wörtlich oder inhaltlich entnommenen Stellen als solche kenntlich gemacht habe.

Graz, am 25. Oktober 2019

Wong Siong Chuong eh

Danksagungen

I would like to express my sincere gratitude to my supervisor, Univ.-Prof. Dr. Klaus Hausegger, in formulating the research topic, for his continuous advice and support in enabling me to conduct and complete the study, for thinking critically and writing the thesis in the scientific way. In addition, I would also like to thank Univ.-Prof. Dr. Hannes Deutschmann for his invaluable expertise during the writing of the thesis.

I would like to thank my colleagues, Dr. Luca de Paoli for his contribution in radiological analysis and Dr. Wolfgang Pipam in the statistical analysis of the project.

Lastly but most importantly, I would like to express my sincere appreciation to my family, for all their support and inspiration in my work and personal life.

Zusammenfassung

Eine retrospective Datenanalyse der Single-Rotation-CT-Angiographie des Halses im Rahmen der CT-Perfusion des gesamten Gehirns - Bewertung eines One-Stop-Imaging-CT-Schlaganfallprotokolls

Einleitung: Die Verfügbarkeit eines 320-Schicht CT Scanners mit 16 cm Z-Achsen Abdeckung bietet die Möglichkeit eine CT Angiographie der Halsgefäße mit nur einer Rotation (single rotation, srCTA) innerhalb des CT Perfusionsprotokolls durchzuführen. Dieses srCTA Protokoll ermöglicht eine schnellere Bildgebung in der Akutabklärung von Schlaganfallpatientinnen und -patienten.

Ziel: Die Machbarkeit der srCTA der Halsarterien zu bewerten, die bei Patientinnen und Patienten mit ischämischem Schlaganfall durchgeführt wurden.

Methoden: 143 Patientinnen und Patienten wurden durch eine einzige Gabe von Kontrast-Mittel (KM) 60 ml mit einem 320-Schicht Volumen CT Scanner untersucht. Die Dichte der Kontrastierung in den Halsgefäßen wurde durch Messung der Hounsfield Units (HU) in den Halsarterien und Halsvenen gemessen. Zusätzlich wurde Beurteilbarkeit der Karotisbifurkation analysiert und mit den Bildern der Digitalen Subtraktionsangiographie (DSA) verglichen. Die Häufigkeit des Auftretens von Artefakten und Gefäßstenosen wurde erhoben.

Ergebnisse: Insgesamt waren im Rahmen der srCTA des Halses die supraaortalen Gefäße bis zum Abgang aus dem Aortenbogen in 58 (40.6%) der Patientinnen und Patienten dargestellt. Der arterielle Abschnitt war dabei in 94.8% (1140/1152) der Gefäße ausreichend kontrastiert (≥ 150 HU). Die Abgrenzbarkeit der Arterien von den Venen war bei 81.3% (915/1126) der Gefäßabschnitte gegeben. In 14.0% (158/1126) der venösen Gefäßabschnitte war jedoch eine höhere Kontrastierung im Vergleich zu den Arterien zu bemerken, was zu einer Verzögerung der srCTA führte. Die Bilder von 95.5% (273/286) der Karotisbifurkationen wiesen eine gute Qualität und Beurteilbarkeit auf. Die Messung des Stenosegrades in der srCTA nach NASCET Kriterien korrelierte signifikant mit der DSA ($R = 0.87$, $p < 0.05$). Bei insgesamt 22.4% (32/143) der Patientinnen und Patienten konnten deutliche Artefakte betroffen, bedingt durch

Zahnprothesen und Metall (10.5%), durch gestautes KM in den Zentralvenen (7.7%) und durch die Schultern (4.9%) beobachtet werden.

Schlussfolgerung: Der Einschluss einer srCTA der Halsgefäße in das bildgebende Protokoll für die Diagnostik von akuten Schlaganfallpatientinnen und -patienten ermöglicht mit nur einer einzigen KM-Gabe die Darstellung der Gefäße in ausreichender Bildqualität, um therapeutische Entscheidungen treffen zu können. Die wesentliche Nachteile sind die mangelnde Abdeckung der supraaortalen Gefäße und mögliche zeitliche Verzögerungen bei der Bildakquisition durch die srCTA.

Abstract

A retrospective analysis of single rotation CTA of the neck in cerebral whole brain CT-Perfusion – evaluation of a one-stop-imaging CT stroke protocol

Introduction: Large volume-CT scanners with 16 cm z-axis single rotation coverage enable joggle-mode scanning of cerebral CT-perfusion (CTP) and single rotation CTA (srCTA) of cervical arteries. The time needed to perform diagnostic imaging in stroke patients could therefore be shortened.

Purpose: Our study aims to evaluate the feasibility of scanning cervical arteries, acquired with srCTA during CTP in ischemic stroke patients.

Methods and Materials: 143 patients were scanned with single contrast medium (CM) injection of 60 ml. Hounsfield Units (HU) of cervical arteries and veins were objectively measured. Carotid bifurcations were analysed qualitatively and also correlated with DSA. Incidence of artefacts and supra-aortic vessels coverage were recorded.

Results: srCTA of the was able to depict the supra-aortic vessels from their origin at the aortic arch in 58 (40.6%) patients. 94.8% (1140/1152) of arterial segments were adequately opacified (≥ 150 HU). Arteries were adequately contrasted compared to veins in 81.3% (915/1126) segments. However the opacification was reversed in 14.0% (158/1126) of the segments, indicating delayed timing of acquisition. 95.5% (273/286) of the carotid bifurcations were of good image quality. Measurement of ICA stenosis in srCTA according to NASCET correlated well with DSA ($R = 0.87$, $p < 0.05$). In 22.4% (32/143) of the patients were the images significantly affected by at least one artefact, mainly from metal/dental implants (10.5%), congested contrast in central veins (7.7%) and shoulder region (4.9%).

Conclusion: srCTA of neck incorporated into cerebral CTP with single CM administration revealed adequate image quality for further decision making in our patient cohort. Main drawbacks were inadequate coverage of supra-aortic arteries and possible delay in timing of the joggle.

Inhaltsverzeichnis

Danksagungen.....	ii
Zusammenfassung.....	iii
Abstract.....	v
Inhaltsverzeichnis.....	vi
Glossar und Abkürzungen.....	viii
Abbildungsverzeichnis.....	x
Tabellenverzeichnis.....	xi
1 Introduction.....	12
1.1 Stroke Epidemiology and Terminology.....	12
1.2 Progress in the Management of Stroke.....	13
1.3 Recent Advances in Stroke Treatment.....	13
1.4 Diagnostic Imaging of stroke patients.....	14
1.5 320-row detector large volume CT.....	15
1.6 Objective.....	16
2 Materials and Method.....	17
2.1 CT-scan protocol.....	17
2.2 Digital subtraction angiography (DSA).....	18
2.3 Patient Population.....	19
2.4 Quantitative analysis.....	21
2.4.1 Measurement of HU at corresponding arteries and veins.....	21
2.4.2 Correlation of srCTA and DSA in the same carotid bifurcation.....	23
2.5 Qualitative analysis.....	24
2.5.1 Coverage of the origins of supra-aortic arteries.....	24
2.5.2 Image quality of the carotid bifurcations.....	26
2.5.3 Artefacts.....	27
2.6 Image analysis.....	27
2.7 Study Protocol.....	28

3	Results.....	29
3.1	Adequacy of coverage of the supra-aortic arteries.....	29
3.2	Quantitative Analysis.....	30
3.2.1	Arterial Segments.....	31
3.2.2	Venous Segments.....	32
3.2.3	Arterial-Venous Attenuation Difference.....	33
3.3	Qualitative Analysis of Carotid Bifurcations.....	35
3.4	Quantitative correlation of proximal ICA stenosis between srCTA and DSA.....	37
3.5	Artefacts.....	40
4	Discussion.....	44
4.1	Adequacy of scan range.....	44
4.2	Comparison to previous studies.....	44
4.3	Timing for Initiation of the Carotid Joggle.....	45
4.4	Correlation between srCTA and DSA.....	46
4.5	Artefacts affecting image quality.....	47
5	Conclusion.....	48
6	References.....	49

Glossar und Abkürzungen

Keywords

- Multidetector computed tomography;
- Brain Ischemia;
- Neck;
- Vascular Diseases;
- Imaging

Keypoints

- Fast treatment decision is needed to preserve salvageable brain in stroke patients and imaging is an important step of the management pathway.
- In Multimodal CT evaluation of acute stroke patients, a large volume CT scanner enables the acquisition of the extracranial CTA through one automated rotation (Joggle mode), in contrast to a continuous spiral scanning in other non-large volume CTs, with the latter requiring extra planning and therefore added time before the actual scan itself.
- Our study results show that a Joggle mode in a large volume CT produces extracranial CTA images of adequate quality with low incidence of artefacts

List of Abbreviations

CCA - Common Carotid Arteries

CM - Contrast Medium

CTA - Computed Tomography Angiography

CTP - Computed Tomography Perfusion

DLP - Dose Length Product

DSA - Digital Subtraction Angiography

HU - Hounsfield Units

ICA - Internal Carotid Arteries

IJV - Internal Jugular Veins

MCA – Middle Cerebral Artery

MIP – Maximum Intensity Projection

MTE - Mechanical Thrombectomy

NASCET – North American Symptomatic Carotid Endarterectomy Trial

NE-CT - Non-enhanced Computed Tomography

PACS – Picture Archiving and Communication System

SEMAR - Single Energy Metal Artifact Reduction

Spiral-MS-CTA – spiral mode multi-slice Computed Tomography Angiography

srCTA - single rotation CTA

SVC - Superior Vena Cava

Abbildungsverzeichnis

Figure 1 Global incidence of stroke by age and sex.....	12
Figure 2 Imaging Pathway for Multimodal CT scanning in stroke patients.....	15
Figure 3 Simplified Schematics of the Carotid Joggle during CTP of 320-row detector Volume CT.....	18
Figure 4 Percentage of patients according to gender.....	19
Figure 5 Incidence of our patient cohort by age group and gender.....	20
Figure 6 Quantitative HU were measured in the Arteries (A1-A9) and Veins (V1-V9) following the locations described in the diagram.....	21
Figure 7 NASCET criteria of measurement for Carotid Artery Stenosis.....	23
Figure 8 Demonstration of the origins of the supra-aortic vessels.....	24
Figure 9 Demonstration of the origins of supra-aortic vessels.....	25
Figure 10 Demonstration of the origins of supra-aortic vessels.....	26
Figure 11 Study Protocol.....	28
Figure 12 Plotchart of the measured Average HU, minimum HU and maximal HU	30
Figure 13 Percentage of aorta and carotid arteries with $HU \geq 150$ (good contrast) and $HU < 150$ (poor contrast).....	31
Figure 14 Differentiation of corresponding carotid arteries and jugular veins.....	33
Figure 15 srCTA images of carotid bifurcations – differences in intraluminal HU.	36
Figure 16 Pseudothrombosis.....	38
Figure 17 Scatterplot Chart for Degree of ICA stenosis in srCTA and DSA according to NASCET methods.....	39
Figure 18 Incidence of artefacts.....	41
Figure 19 SEMAR.....	42
Figure 20 Pseudodissection.....	43

Tabellenverzeichnis

Table 1 Coverage of Origin of Supra-aortic Arteries_____	29
Table 2 Qualitative Analysis of srCTA neck vessels_____	35
Table 3 Quantitative Analysis of degree of ICA stenosis in srCTA and DSA using NASCET methods_____	37
Table 4 Incidences of Number of Significant Artefacts Per Patient_____	40

1 Introduction

1.1 Stroke Epidemiology and Terminology

Stroke is defined by the World Health Organisation (WHO) in 1980 as “rapidly developing clinical signs of focal (or global) disturbance of cerebral function, lasting more than 24 hours or leading to death, with no apparent cause other than that of vascular origin” (1). It is the second leading cause of global mortality and causes great disability worldwide (2). The incidence of stroke increases with age (3) (see Figure 1). It can be divided into two types, the majority of which are ischemic (87%) and rest of which are hemorrhagic stroke (13%) (4).

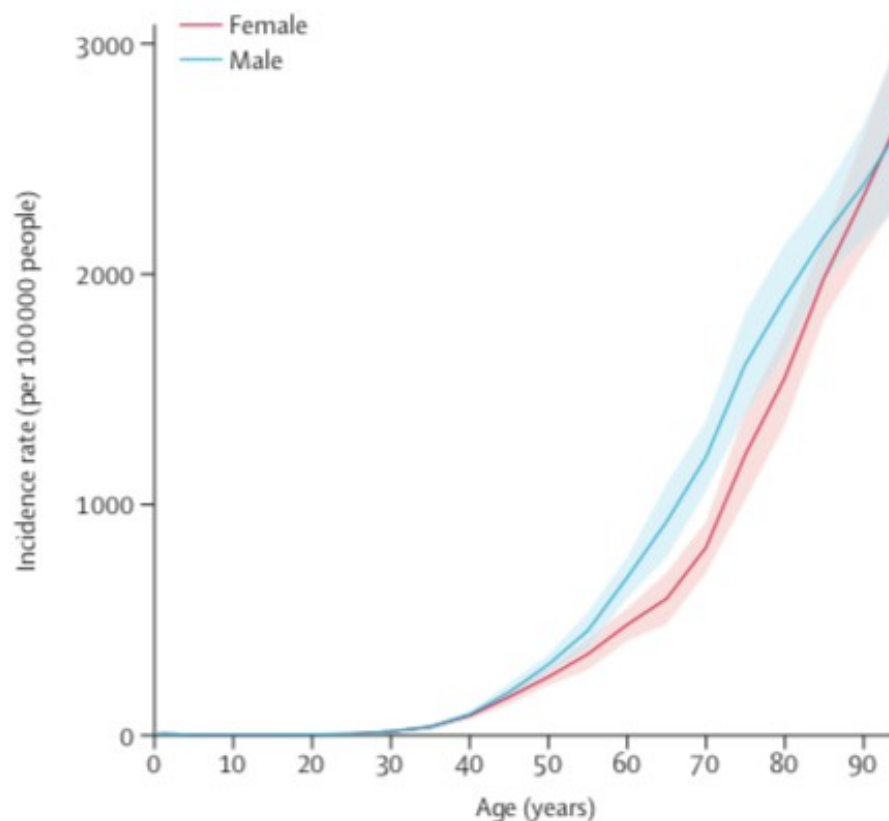


Figure 1 Global incidence of stroke by age and sex.

(Note: Taken from (3) with an Open Access article under the CC BY 4.0 license).

The symptoms of stroke were already recorded by Hippocrates, the father of medicine, since the ancient times from nearly 2400 years ago. At that time however, it was named as “apoplexy”, meaning “struck down by violence” in Greek. Only with the emergence of cadaveric examination in the 17th century, was the correct understanding of “apoplexy” identified. The term “stroke” was first used in the year 1689, but not until 1968 was adopted into ICD-9 (5).

1.2 Progress in the Management of Stroke

In the early 1900s, the treatment of stroke patients were focused on its aftermath, namely rehabilitation. This is because in most patients, the permanent disability is irreversible. Since the description of stroke by Hippocrates nearly 2500 years ago, only in the last 50 years, the treatment strategy of stroke begin to advance substantially. These started with primary and secondary prevention strategies through Carotid Endarterectomy (6) (1950s) and aspirin (7) (1970s). Nevertheless, these treatments do not actually target the intracranial vascular thrombus itself.

1.3 Recent Advances in Stroke Treatment

Treatment strategies directed towards the intracranial vascular thrombus started with clot-buster tissue plasminogen activator (8) (1990s) and clot-retrieving mechanical thrombectomy (9) (since 2014/2015). These two treatment options could for the first time in the history of stroke management, potentially reverse or limit the damage of cerebral ischemia, by reestablishing flow after recanalising the occluded intracranial arteries.

However, early diagnosis and prompt initiation of acute stroke treatment are essential in determining patient outcome, as these treatments target the salvageable reversible area of cerebral ischemia, the penumbra area. In a patient who suffered a large vessel stroke, 1.9 million neurons are irreversibly

lost every minute (10). Therefore, time is of essence, hence the phrase “time is brain” (11).

1.4 Diagnostic Imaging of stroke patients

A crucial part of intrahospital stroke management pathway includes establishing diagnosis and estimating size of infarcted tissue against the penumbra. These information could be derived from diagnostic imaging. With the advancement of technology, newer methods of diagnostic imaging continues to be developed. A multimodal CT protocol for stroke incorporates several methods of CT scanning, providing anatomical and functional informations (12). These are explained further as below.

Non-enhanced Computed Tomography (NE-CT) and Computed Tomography Angiography (CTA) are primary imaging modalities in the evaluation of patients with acute ischemic stroke (13,14). They enable exclusion of intracerebral hemorrhage, diagnosis of cerebral infarct and detection of large vessel occlusion. In numerous centers, Computed Tomography Perfusion (CTP) is also included in the imaging protocol for acute stroke (15–17), enabling the estimation of irreversible infarct core, area of reversible penumbra and state of vascular collateralisation. This information is essential for establishing the indication for revascularization, specifically Mechanical Thrombectomy (MTE). When MTE is in the therapeutic perspective, it is desirable to know the angio-anatomical status of the carotid and vertebral arteries. Severe kinking and stenoses may strongly influence the complexity of MTE.

In the traditional multimodal stroke imaging protocol, where the cerebral CTP and arch-to-vertex spiral multi-slice CTA (spiral-MS-CTA) are performed separately, double Contrast Medium (CM) application is necessary (18) (see Figure 2).

1.5 320-row detector large volume CT

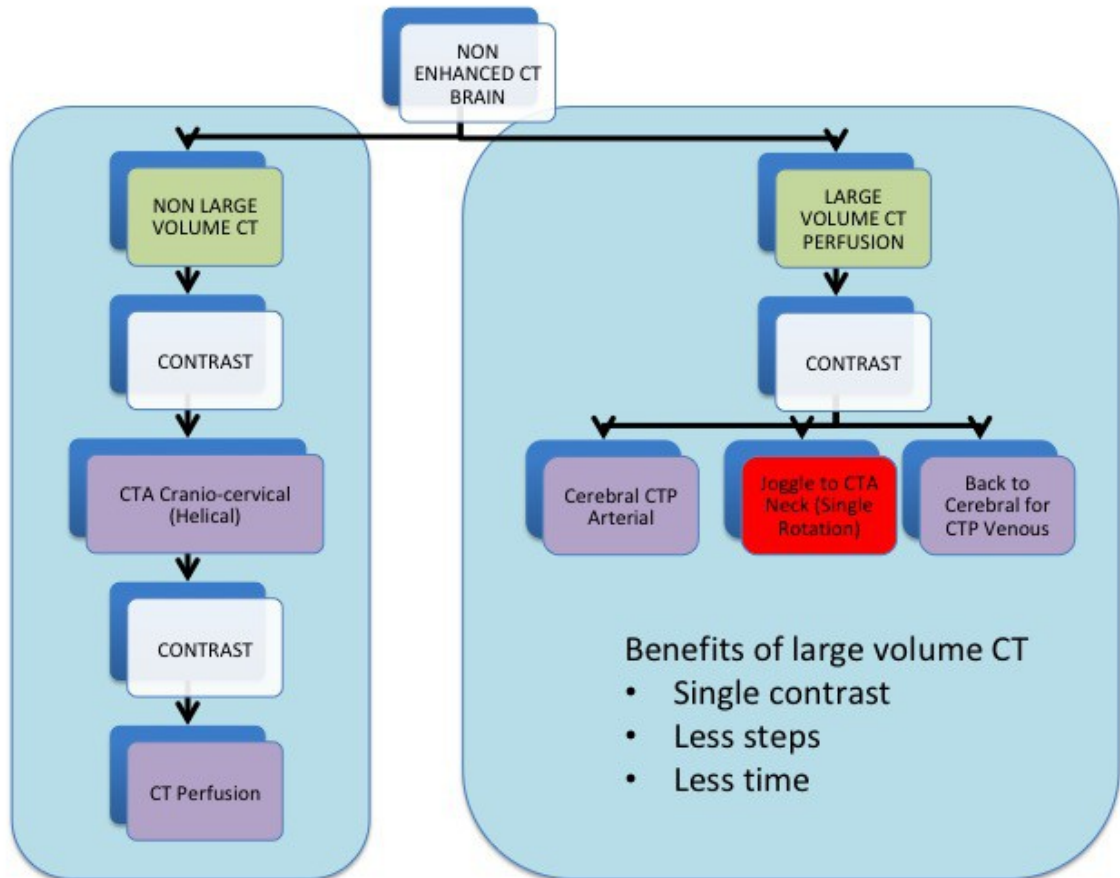


Figure 2 Imaging Pathway for Multimodal CT scanning in stroke patients. Differences in amount of steps and order of sequences between non-large-volume CT and large volume CT Scan. Large volume CT with Carotid Joggle requires less steps and less contrast media.

320-row detector volume CT scanners cover z-axis volume as large as 16 cm in a 0.5 sec single rotation. With volume scanners it has become possible to acquire a whole brain CTP and CTA of the cervical arteries with a single CM application. In a non-large-volume CT, the CTP and CTA are acquired separately with the additional step and extra time for planning and contrast media injection prior to each scans.

On the other hand, a snap-shot single rotation CTA (srCTA) of the cervical artery is automatically taken in the midst of CTP acquisition in the 320-row detector large-volume CT machine (see Figure 2). The scanning protocol in large-volume CT involves fewer steps and planning, therefore saving time.

However, the exposure factor and the scan range in srCTA neck is fixed and this may hamper image quality. It is the aim of this study to evaluate the feasibility and image quality of srCTA of the cervical arteries acquired during CTP. The perfusion scan is not in the scope of this analysis.

1.6 Objective

We aim to analyse the images of joggle mode srCTA neck done during early dural venous phase of cerebral CTP scan. Specifically, the following aspects will be considered:

- a) Ability to demonstrate the origin of all supra-aortic arteries
- b) Image quality of srCTA neck in quantitative and qualitative terms.
- c) Correlation of image quality between srCTA and DSA of the same carotid bifurcation.
- d) Incidence of artefacts.

2 Materials and Method

2.1 CT-scan protocol

srCTA of the cervical arteries and CTP were acquired with a 320 row detector CT scanner (Aquilion ONE Vision Edition; Canon (formerly Toshiba); Japan).

The cranial and cervical scan ranges were prescribed via 2 x 16 cm biplanar scanograms, beginning from the skull vertex. The cervical scanogram was automatically set inferior to the cranial scanogram, with an overlap of 1 cm. Single Energy Metal Artifact Reduction (SEMAR) was manually activated if metallic objects were detected in the scanogram.

Via a large antecubital vein, 60 ml of CM (350 mg I/ml Iomeprol Bracco GmbH) were injected at flow rate of 5 ml/s, followed by 30 ml saline bolus at 5 ml/s. Scanning (0.5 sec/80kV/400 mA) was started with a stationary rotation at the head region, 7 sec. after the beginning of the CM injection, for bone masking of subsequent scans. Perfusion scanning (0.5 sec./80 kV/200 mA) was started at 12 sec. after contrast injection has been initiated, in 2 seconds intervals.

Progressive opacification at the level of midsection of brain was displayed on the CT-console. When early contrast filling of the dural veins was seen, an on-screen switch was manually triggered by the operator and the table was moved to the cervical region where an srCTA of the neck was acquired (0.5 sec./80kV/400mA). Immediately thereafter the table automatically moved back to the cranial position and scanning continued with the rest of the perfusion study, with scan intervals of 2 seconds for 16 seconds and thereafter in 5 seconds intervals for 20 seconds. Depending on cardiac output which influences the arrival of contrast in the brain, the whole CTP-srCTA Protocol typically takes around 60 seconds. Please see Figure 3 for a simple schematic of the srCTA protocol.

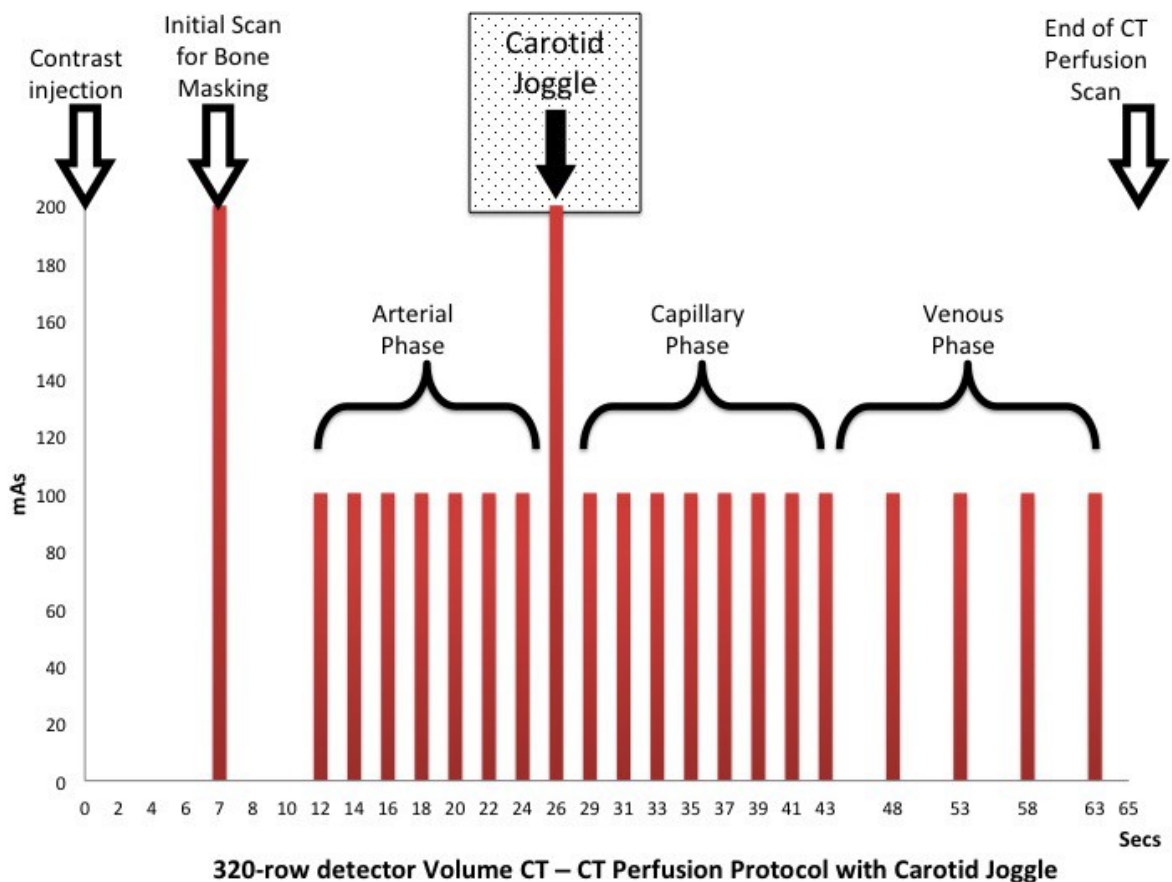


Figure 3 Simplified Schematics of the Carotid Joggle during CTP of 320-row detector Volume CT

Adaptive iterative reconstruction was used to process the CT images. srCTA neck images were reconstructed axially at slice thickness and reconstruction interval of 1.0 mm and were available as a separate dataset.

2.2 Digital subtraction angiography (DSA)

Carotid bifurcation DSA was acquired on a biplane state-of-the-art angiography system (Siemens AXIOM Artis mB, Germany) as a part of MTE with the tip of the catheter in the distal Common Carotid Arteries (CCA). CM (Iodixanol 270 mg I/ml;GE Healthcare) was manually injected and DSA of the carotid bifurcations were acquired in frontal and lateral projections.

2.3 Patient Population

This was a retrospective study. A local PACS search of patients who had srCTA for suspected stroke in the 58 months from 1st Oct 2014 to 31st July 2019 were included into the study. Excluded were patients who are pregnant or in the pediatric age group (0-18 years of age), not only due to radiation burden but also due to changes in flow dynamics of contrast media and body build. Local Ethics Commission approval (A 29/19) was obtained for this study.

Due to the nature of retrospective study, informed consent from the patients could not be obtained. The data of the included patients were nevertheless anonymised before analysis.

A total of 143 patients (male 73, female 70) were included into the study (see Figure 4).

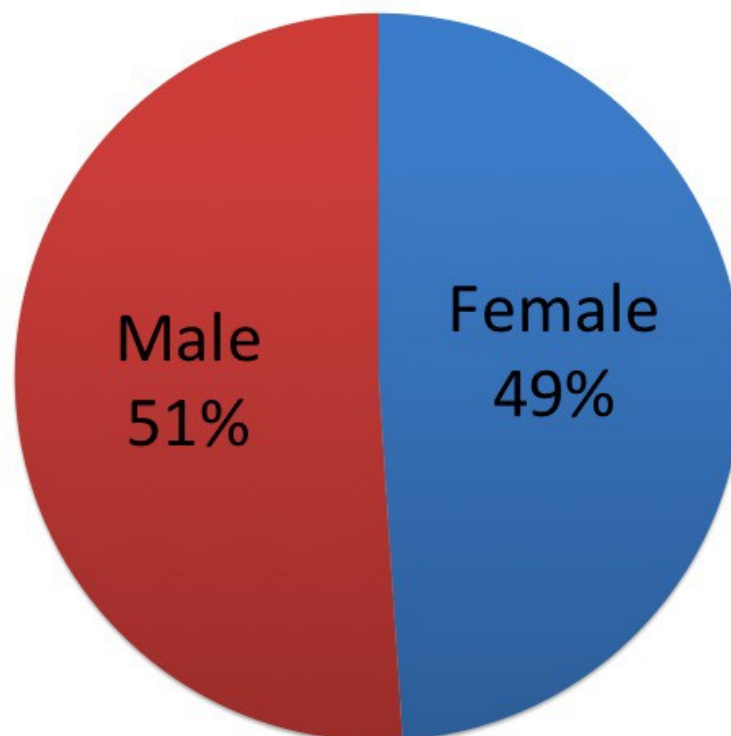


Figure 4 Percentage of patients according to gender

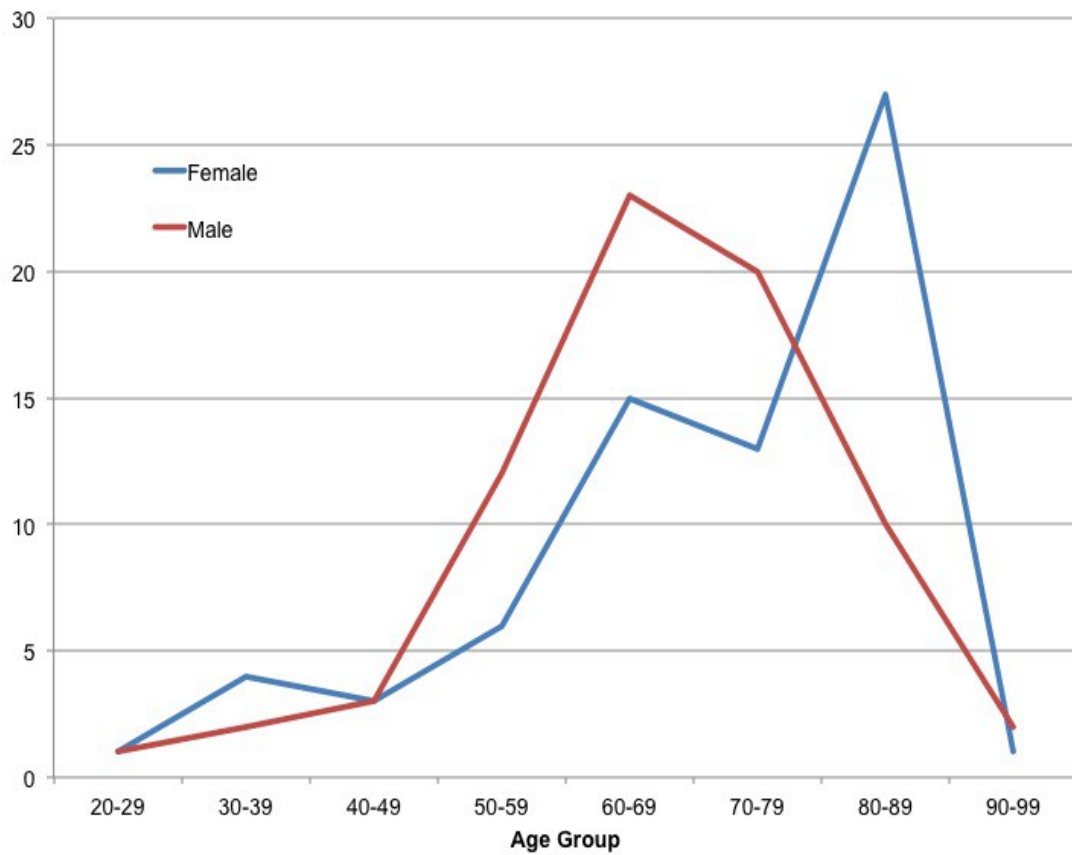


Figure 5 Incidence of our patient cohort by age group and gender

The average age of the patients is 68.6 years with range from 24 to 91. In our cohort, male patients presenting with stroke tends to be more younger than female patients (see Figure 5).

2.4 Quantitative analysis

2.4.1 Measurement of HU at corresponding arteries and veins

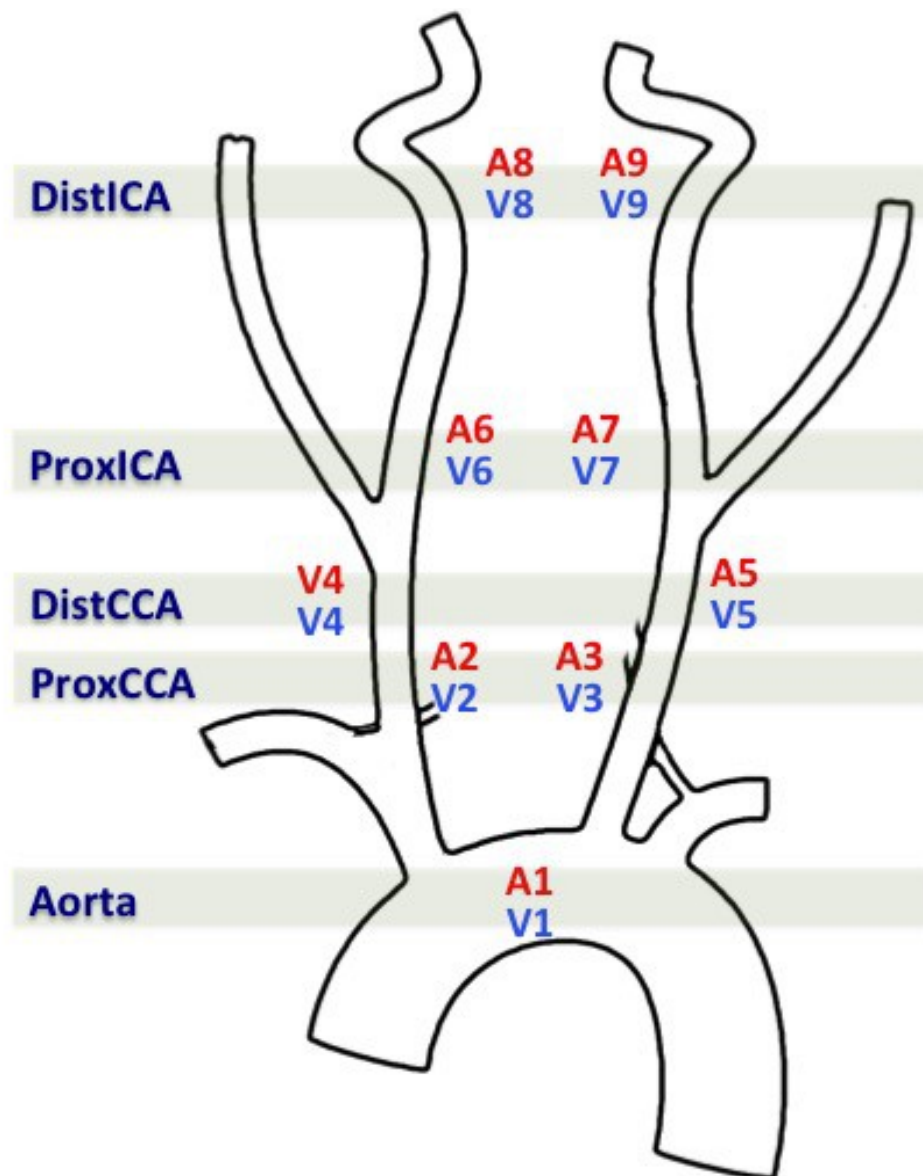


Figure 6 Quantitative HU were measured in the Arteries (A1-A9) and Veins (V1-V9) following the locations described in the diagram.

The mean, minimum and maximum Hounsfield Units (HU) were measured at 9 locations (see Figure 6), namely at the aorta (just below brachiocephalic trunk), proximal bilateral CCAs (level of inferior aspect of cricoid cartilage), distal bilateral CCAs (level of hyoid bone or just below carotid bifurcations, whichever more inferior), proximal bilateral Internal Carotid Arteries (ICAs) (just above carotid bifurcations) and distal bilateral ICAs (level of anterior arch of C1).

The Region of Interest (ROI) for measuring HU was drawn as large of possible, taking care to avoid vessel wall and calcifications. The same HU parameters were measured in the corresponding veins [Superior Vena Cava (SVC) and Internal Jugular Veins (IJVs)].

In accordance with Kim et al. (19),

- a) to determine optimal CTA, arterial attenuation values of ≥ 150 HU were used.
- b) discrimination of arteries from corresponding veins was good if they had difference attenuation of ≥ 50 HU.
- c) The numbers of segments fulfilling these two criteria were counted and their incidence calculated.

2.4.2 Correlation of srCTA and DSA in the same carotid bifurcation.

srCTA was correlated to DSA at the proximal ICA, measured by the degree of stenosis in both modalities by the NASCET criteria (see Figure 7). 2 measurements respectively in the same sites in srCTA and DSA were performed as follows;

- a) A = luminal diameter of ICA after the carotid bulb where the arterial wall becomes parallel
- b) B = luminal diameter at the site of maximal narrowing in the proximal ICA
- c) The degree of stenosis was thereafter calculated as follows,
 $(A-B)/A \times 100\%$.
- d) The degree of stenosis was assigned as 0% when there is no stenosis and 95% in cases of no flow, or string of contrast flow into the ICA.

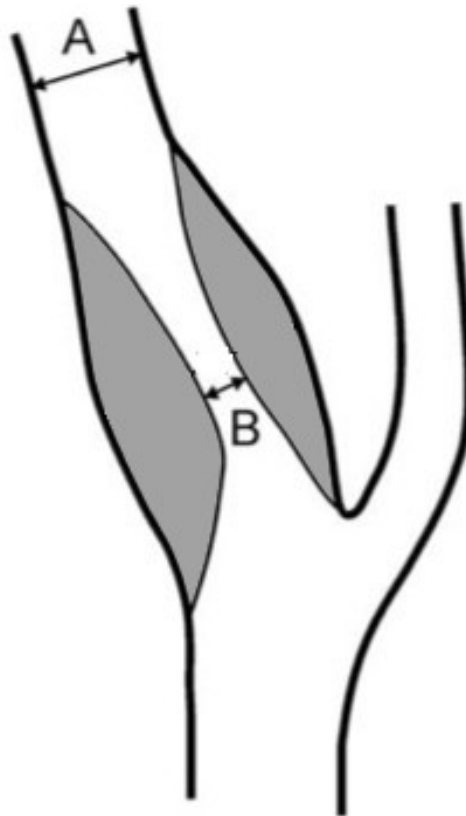


Figure 7 NASCET criteria of measurement for Carotid Artery Stenosis.

Measurements was performed for stenosis in the Internal Carotid Artery in the srCTA and DSA for the same patient.

2.5 Qualitative analysis

2.5.1 Coverage of the origins of supra-aortic arteries

Visual assessments were performed for the following criteria:

Adequacies of coverage of the cervical arteries beginning from the aortic arch whereby the origins of the three large supra-aortic arteries were evaluated. Scoring from 0-2 were applied;

- a)** Score 0 – all three supra-aortic vessel origins outside the scan range (see Figure 8).
- b)** Score 1 – at least one supra-aortic vessel origin in the scan range (see Figure 9),
- c)** Score 2 - all three supra-aortic vessels origins included in the scan range (see Figure 10).

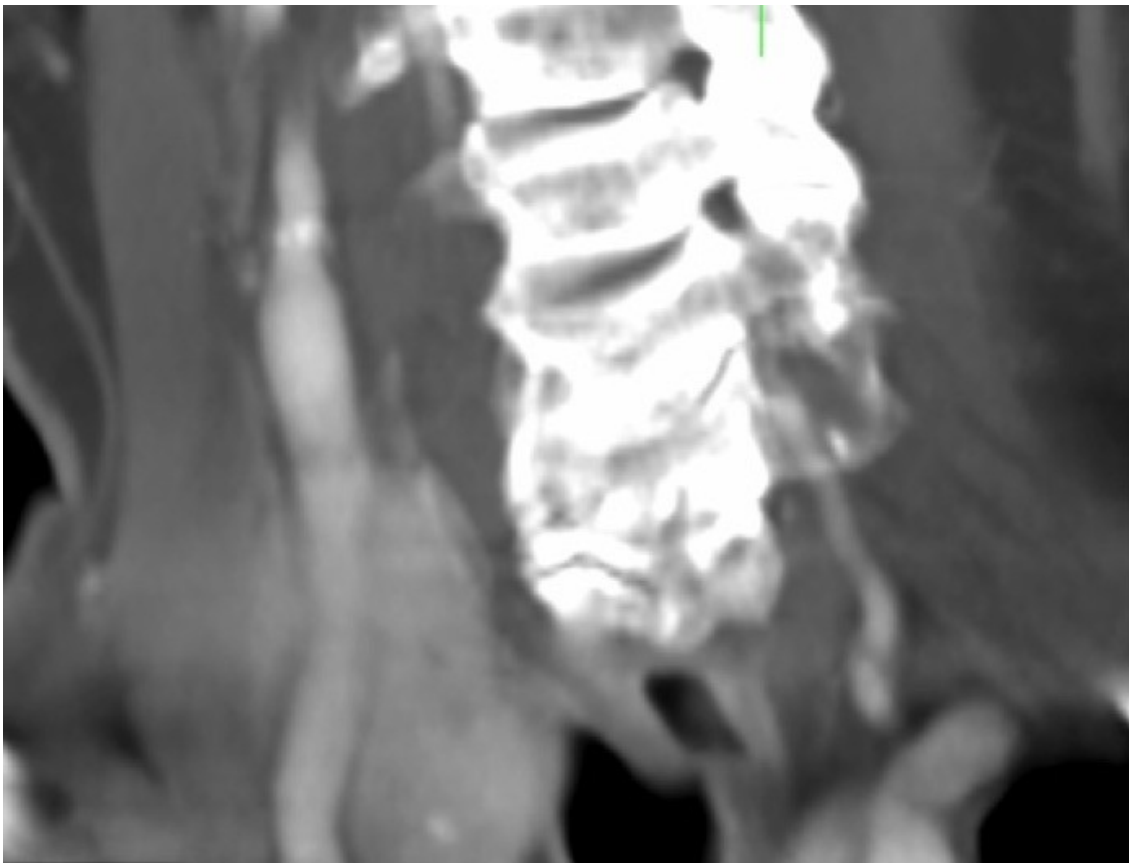


Figure 8 Demonstration of the origins of the supra-aortic vessels.

In this srCTA image, all supra-aortic vessel origins are outside of the scan range.

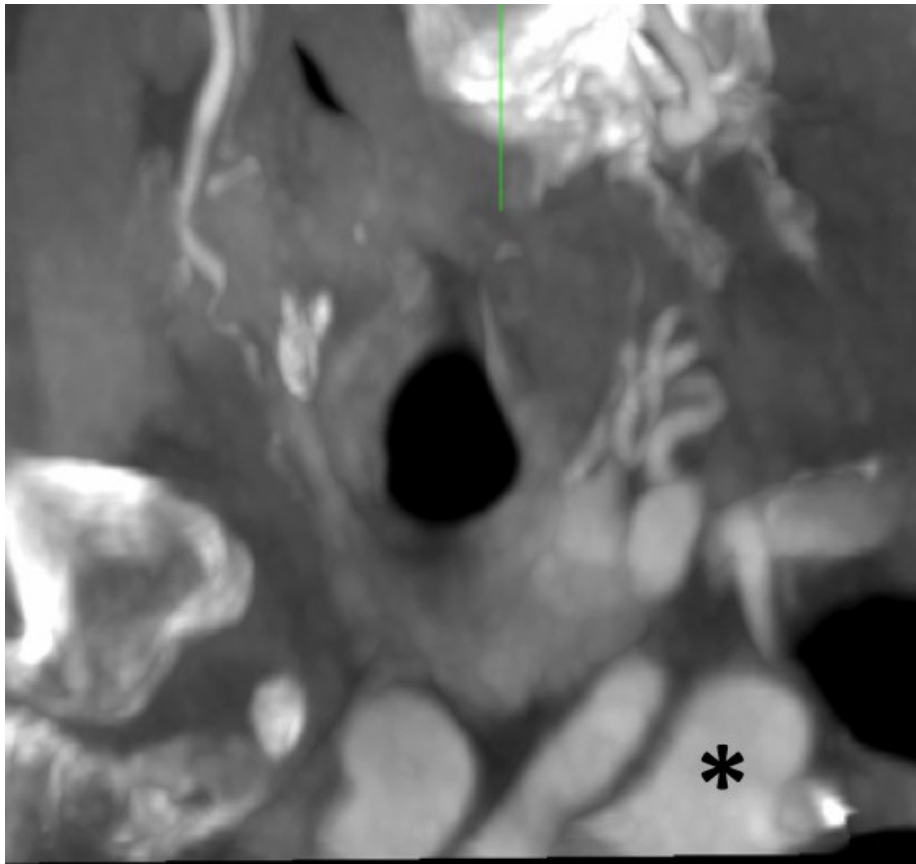


Figure 9 Demonstration of the origins of supra-aortic vessels.

In this srCTA image, only the left subclavian artery origin was demonstrated with (*). The origins of brachiocephalic artery and left common carotid artery were not depicted.

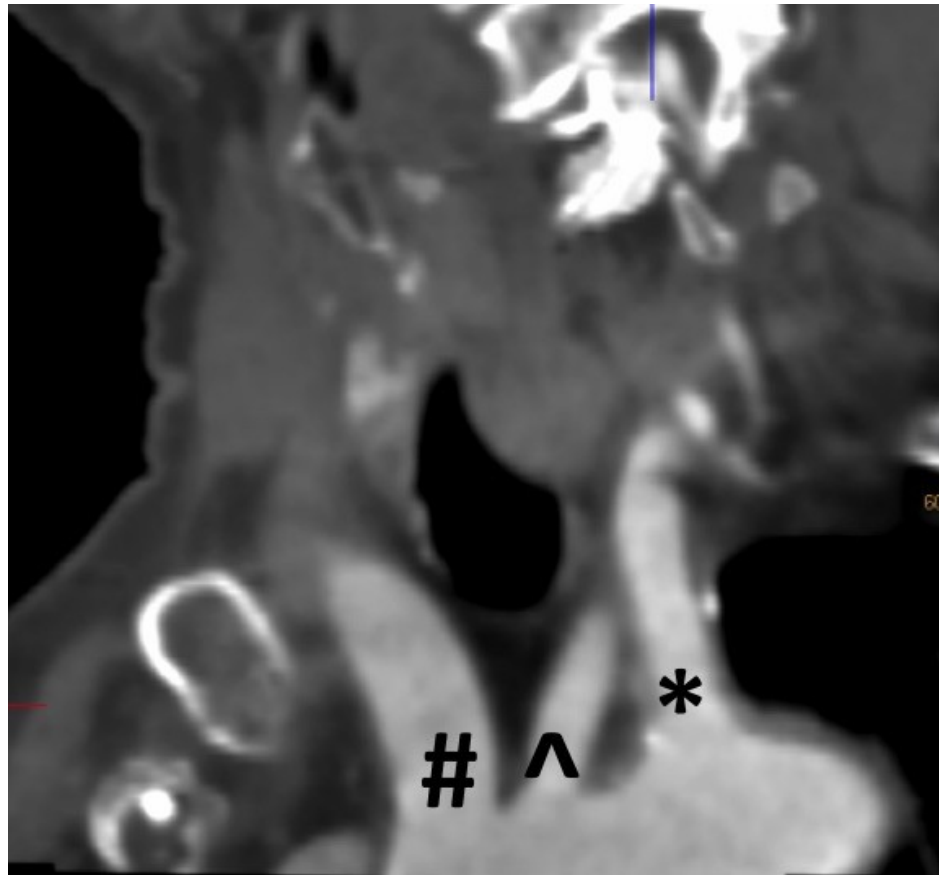


Figure 10 Demonstration of the origins of supra-aortic vessels.

In this srCTA image, all supra-aortic vessel origins were within the scan range. The origins of brachiocephalic artery (#), left common carotid artery (^) and left subclavian artery (*) could be identified.

2.5.2 Image quality of the carotid bifurcations

Subjective assessments of srCTA at the carotid bifurcations. The following scores were applied:

- a) Score 0 - inadequate for planning therapy,
- b) Score 1 – poor quality but adequate for therapy planning,
- c) Score 2 – good diagnostic quality.

2.5.3 Artefacts

Presence of artefacts in the srCTA were due to

- a) shoulders due to photon starvation,
- b) metallic hardware or dental streak,
- c) patient movement,
- d) streak artefacts related to residual injected contrast in central veins,
- e) reflux of contrast material into small neck veins and
- f) flow related artefacts.

The incidences of artefacts were rated as follows:

- a) Yes – image severely obscured by artefact, inadequate for planning therapy,
- b) Mild – image partially obscured by artefact, but adequate for therapy planning,
- c) No – no artefact.

2.6 Image analysis

Images from srCTA neck were read at a state-of-the-art radiological reporting workstation. These were available in 1 mm slices and in Maximum Intensity Projection (MIP). Free multiplanar manipulation was allowed during the analysis. Quantitative values and measurements of proximal ICA stenosis following NASCET criteria were measured and determined by the first author.

The qualitative image and artefacts interpretations were evaluated independently by one senior interventional neuroradiologist (K.A.H) and 2 experienced radiologists (SC.W and L.DiP). Differences were resolved by consensus.

Correlation of ICA stenosis between srCTA and DSA was analysed with the Spearman Correlation Test using SPSS version 18. A P value of less than 0.05 was considered to be statistically significant.

2.7 Study Protocol

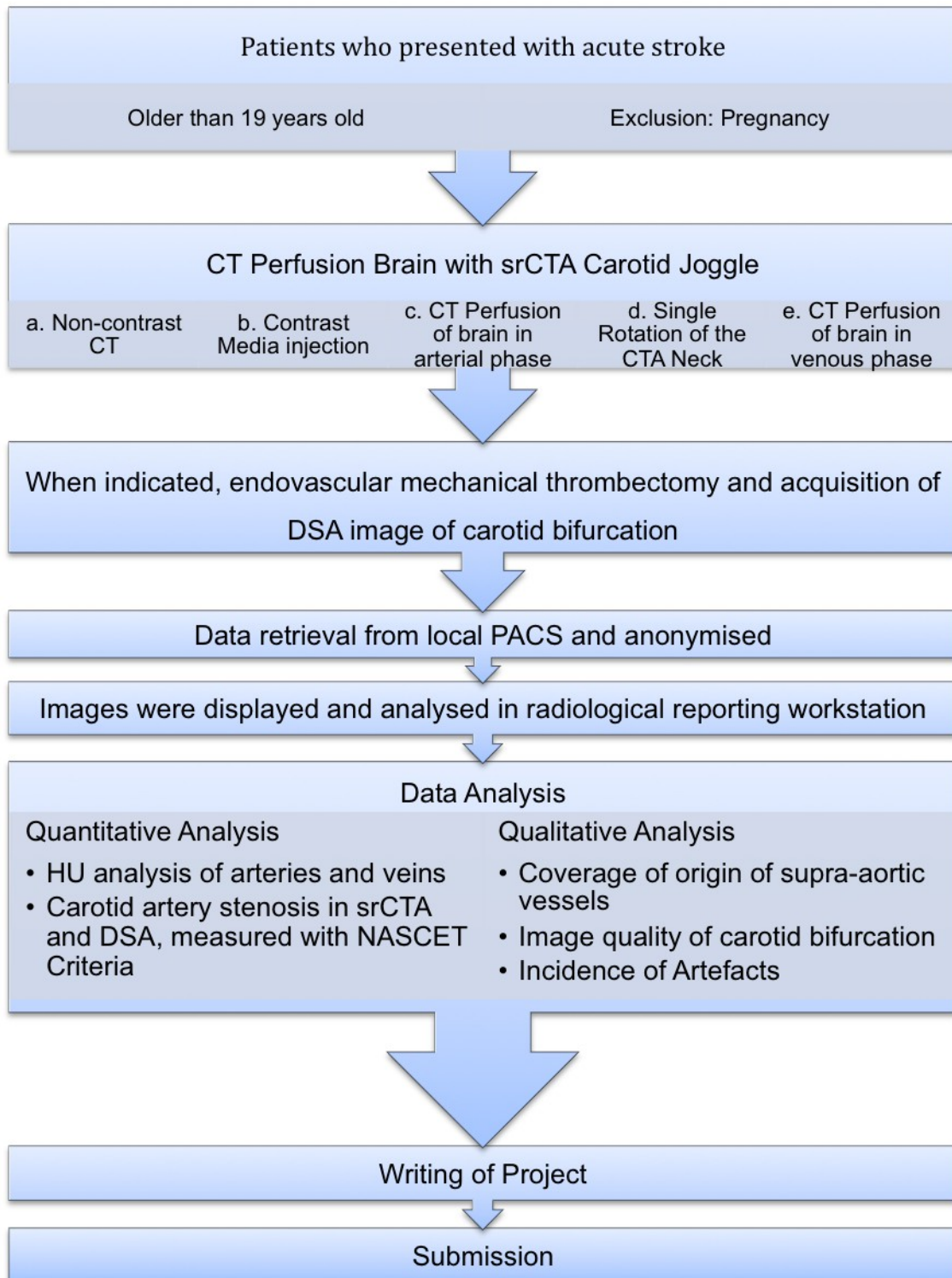


Figure 11 Study Protocol

3 Results

3.1 Adequacy of coverage of the supra-aortic arteries

Inclusion of supra-aortic artery origins	No of supra-aortic vessels (N)	%
All vessels	58	40.6
Partial	16	11.2
None	69	48.3
Total	143	100

Table 1 Coverage of Origin of Supra-aortic Arteries

58/143 (40.6%) patients had srCTA which completely included the origins of major supra-aortic arteries. In 16 (11.2%) patients, only one or two vessel origins were covered and in 69 (48.3%) patients, the inferior margin of srCTA neck scan was too superior to the aortic arch.

3.2 Quantitative Analysis

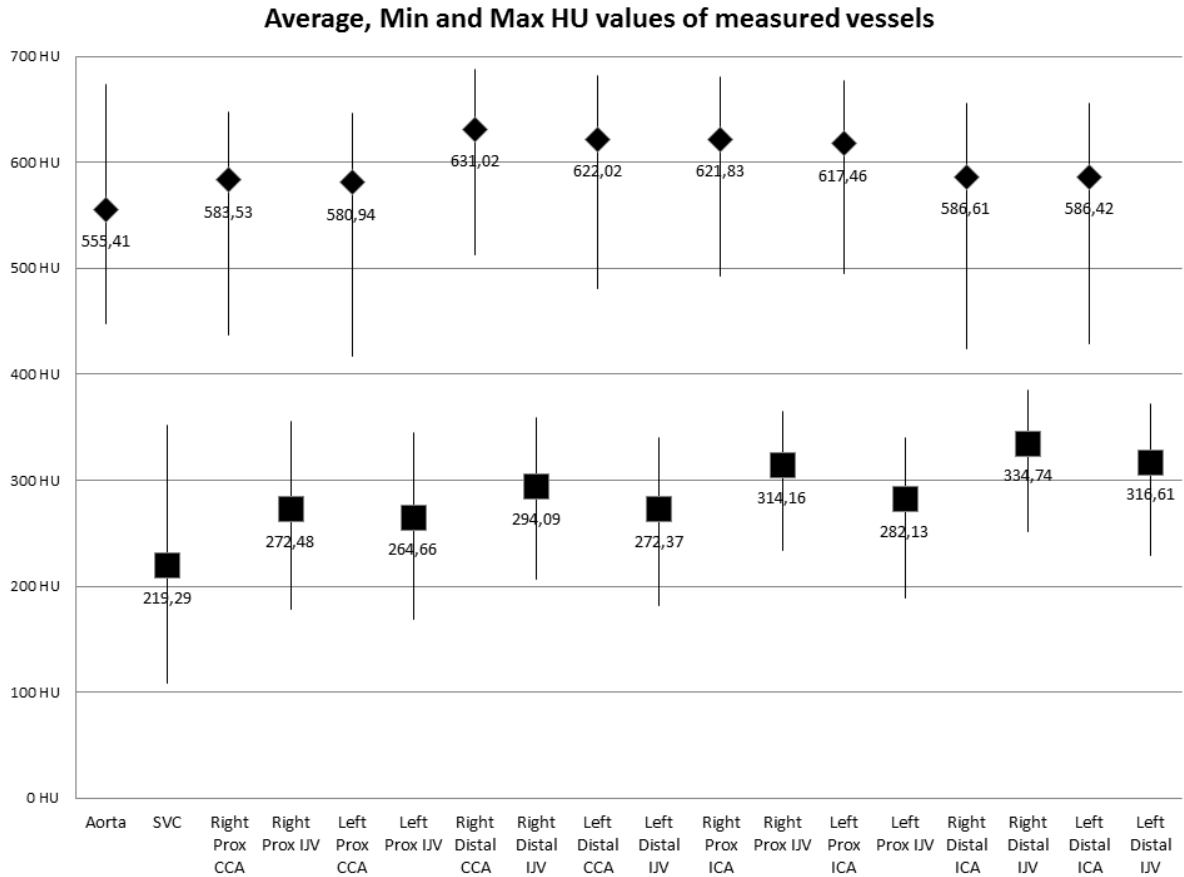


Figure 12 Plotchart of the measured Average HU, minimum HU and maximal HU

Measured HU of the arteries and veins respectively. Note the slightly higher HU of the arteries surrounding the carotid bifurcations, namely distal CCAs and proximal ICAs.

Due to differences in coverage of arch of aorta, a total number of 1202 vascular segments were potentially available for quantitative analysis (58 patients with 9 segments and 85 patients with 8 segments).

3.2.1 Arterial Segments

In 1152 arterial segments the actual HU measurement was possible, with average HU value of 575.2 (SD 43.9, minimum -21.9 HU, maximum 1911 HU). The sole arterial segment with negative HU value was due to a calcified thyroid nodule causing beam hardening artefact in the distal CCA. The unmeasurable 50 segments were due to no flow in ICAs, either from occlusion in the proximal ICA or occlusion in the distal arteries. See Figure 12 for further information for individual arteries.

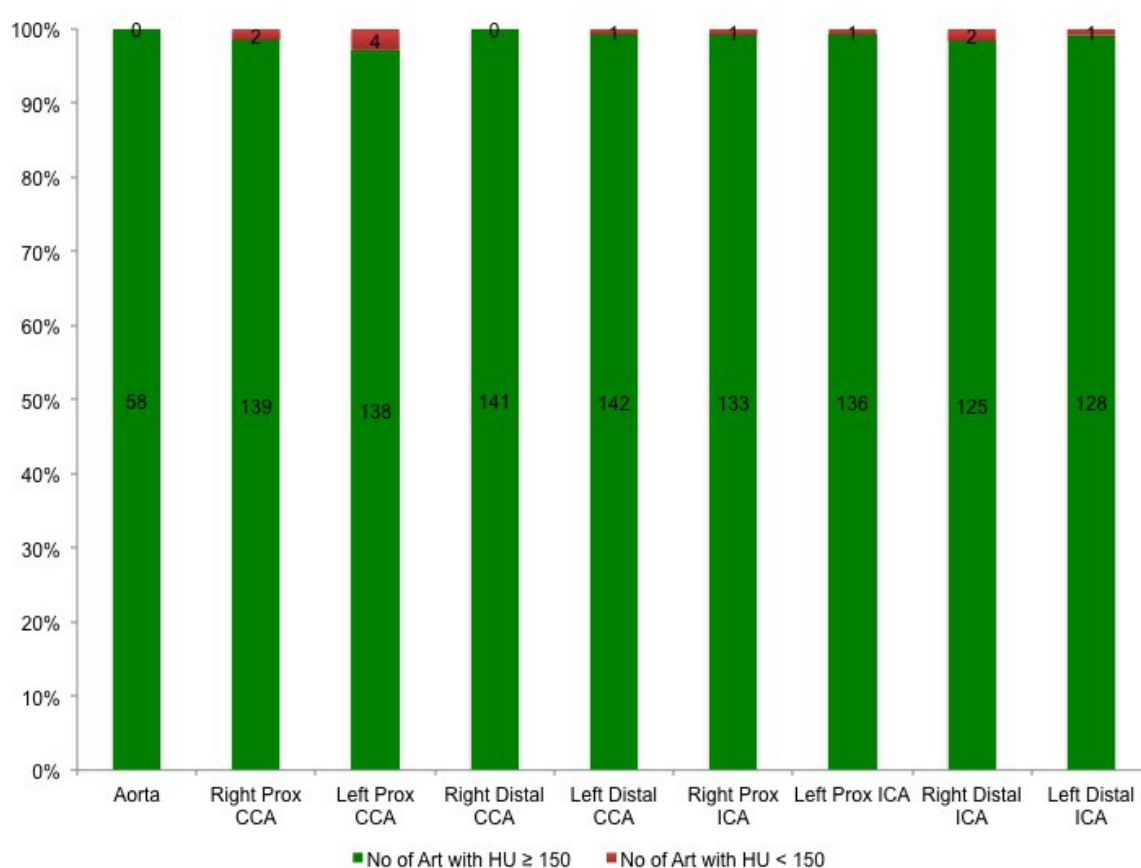


Figure 13 Percentage of aorta and carotid arteries with HU ≥ 150 (good contrast) and HU < 150 (poor contrast).

There were 1140 (94.8%) arterial segments with average HU values ≥ 150 . 12 arterial segments had average attenuation of < 150 HU. The individual segments are shown in Figure 13. These were located in proximal CCA (n=6), distal CCA (n=1), proximal ICA (n=2) and distal ICA (n=3). The average contrast attenuation and number of arterial segments with HU values ≥ 150 were also the highest at distal CCA and proximal ICA, specifically around the region of carotid bifurcation (see Figure 12).

3.2.2 Venous Segments

1169 venous segments were evaluated with mean HU value of 290.5 (SD 34.0, minimum 54, maximum 967). 33 segments were non-evaluable due to inhomogeneous contrast opacification. In 12 segments, this was due to inflow of non-contrasted blood from side branches into the IJV. 10 segments had dense CM in dependent part of IJV, 9 segments had dense CM due to venous reflux from contrast injection and 2 segments had dense CM upstream from a central venous catheter in the neck. Four patients had central venous catheters, but only in one patient there was contrast stasis upstream. This stasis was probably related to the catheter placement, as there was no anatomical stenosis in the affected IJV and no stasis in the contralateral IJV. See Figure 12 for further information regarding individual veins.

3.2.3 Arterial-Venous Attenuation Difference

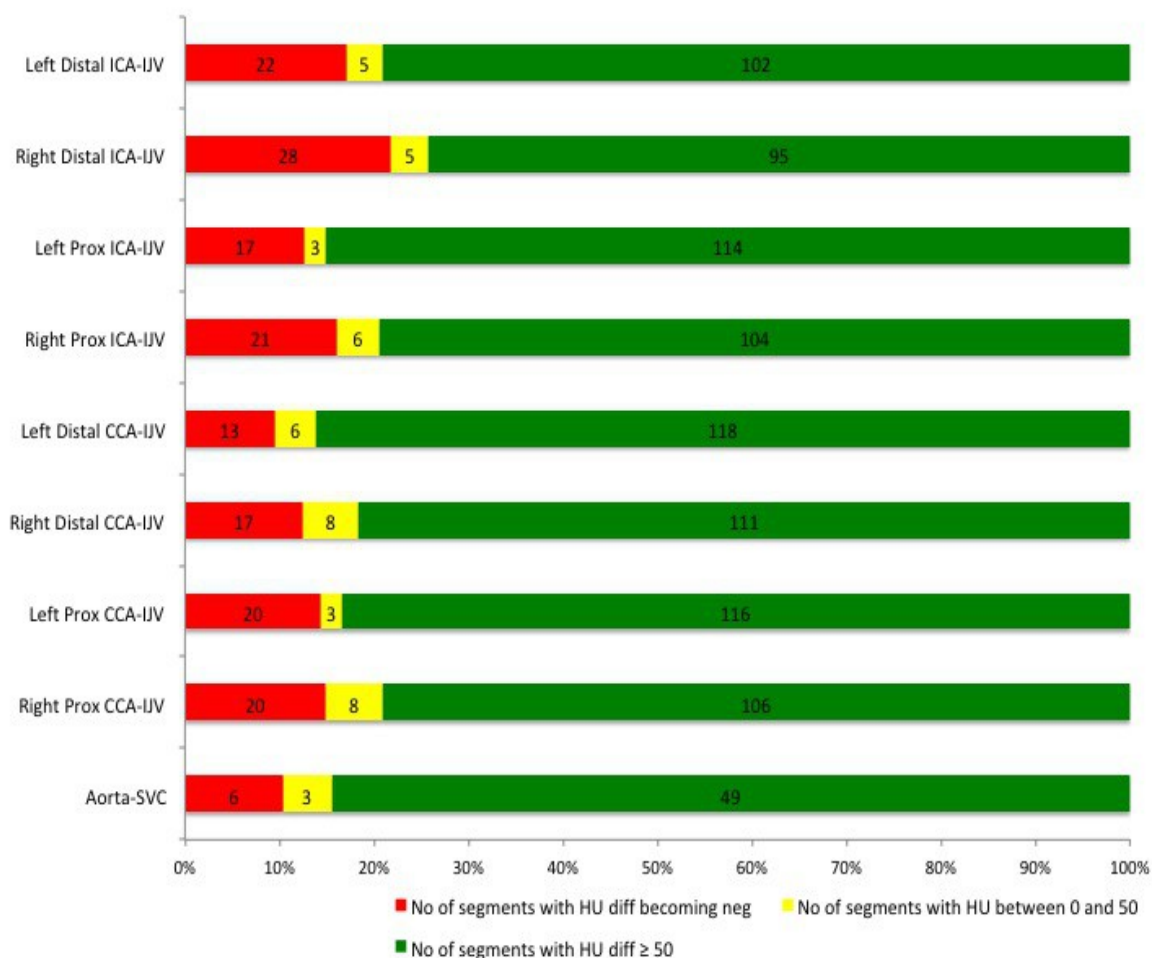


Figure 14 Differentiation of corresponding carotid arteries and jugular veins.

The differentiation were calculated mathematically by HU artery minus HU vein, and categorized in percentage as (a) more than 50 HU – good differentiation, (b) between 0 and 50 – poor differentiation and (c) negative HU – reversal of HU (more contrast in corresponding veins than arteries, indicating delay in imaging)

In 1126 segments the difference of HU attenuation in arterial and corresponding venous segments were calculated, the difference in HU of corresponding segments are shown in Figure 14. There were 915 (81.3%) segments where the arterial segment was ≥ 50 HU compared to the corresponding venous segment. In 211 (18.7%) segments the difference was < 50 HU.

Of these 211 segments, 164 (14.6%) segments had negative attenuation differences, meaning that the attenuation in the veins was higher than in the corresponding arteries. This reversal (more contrast in vein than artery) implies that there was delay in srCTA acquisition, except for aorta-SVC (n=6) segment, where more contrast in the SVC was due to CM injection. Excluding the aorta-SVC segment, negative attenuation difference was noted in 158 (14.0%) segments.

3.3 Qualitative Analysis of Carotid Bifurcations

Visual Analysis of Carotid bifurcations in srCTA (see Table 2)

Quality on srCTA	Right carotid bifurcation	Left carotid bifurcation	Total	%
Non diagnostic image quality (Score = 0)	1	2	3	1.0
Poor image quality but adequate for therapy planning (Score = 1)	5	5	10	3.5
Good diagnostic image quality (Score = 2)	137	136	273	95.5
Average score	1.95	1.94		

Table 2 Qualitative Analysis of srCTA neck vessels

286 carotid bifurcations were visually analysed. Of three possible scores (0-2), a favorable average score of 1.9 was obtained. Also, 273/286 (95.5%) of the carotid bifurcations had good diagnostic image quality.

13 patients had poor visualization of carotid bifurcations due to presence of vascular calcifications creating beam hardening artefact. Of these, 10 carotid bifurcations were adequate for therapy planning (score 1) as there was adequate intraluminal contrast (Figure 15A). However, in 3 carotid bifurcations, as there was insufficient intravascular contrast, causing difficulty or false assessment (Figure 15B).

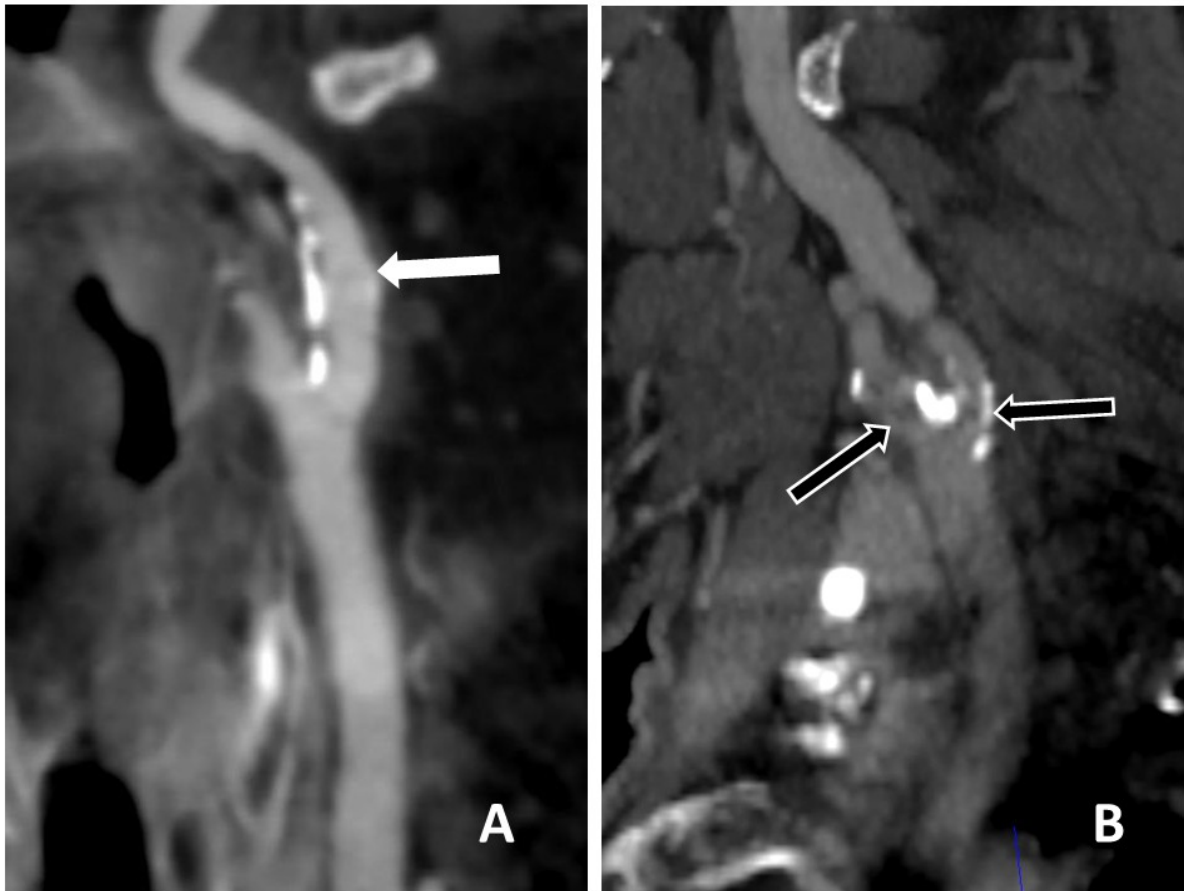


Figure 15 srCTA images of carotid bifurcations – differences in intraluminal HU

srCTA images of carotid bifurcations in a 66 years old patient (**Image A**) and a 70 years old patient (**Image B**). The images are in coronal or curved reconstructed coronal sections. In Image A, average HU of intraluminal contrast measured around 500. In Image B, average HU of intraluminal contrast measured around 200 (meaning that the intraluminal contrast in the carotid artery in image B is much lower compared to the intraluminal contrast in Image A). Maximal HU of calcified wall plaques in both Images measured 1200. Both images show streak artefacts (white arrow in Image A and black arrow with white outline in Image B) from the calcified wall plaques casted into the lumen of both carotid arteries. The streak artefacts are however darker in Image B because there are lesser intraluminal contrast and these may mimic thrombus in the carotid arteries in Image B.

3.4 Quantitative correlation of proximal ICA stenosis between srCTA and DSA

Degree of Stenosis	srCTA	%	DSA	%
0-49% (mild)	45	58.4	49	63.6
50-69% (moderate)	4	5.2	6	7.8
70-99% (severe)	28	36.4	22	28.6
Total	77	100	77	100

Table 3 Quantitative Analysis of degree of ICA stenosis in srCTA and DSA using NASCET methods

77 patients who had images of the same carotid bifurcations on srCTA and DSA were evaluated for the proximal ICA stenosis according to NASCET methods. The majority of patients have mild stenosis (see Table 3).

In srCTA, 6 (7.8%) patients were presumed to have complete stenosis, due to non flow of contrast media downstream to the carotid stenosis. Using DSA as the gold standard, however, only 5 of these were subsequent found to have moderate or no stenosis in DSA. Only one patient with discordance had true high grade proximal ICA stenosis in DSA when compared to srCTA (see Figure 16). These discordances were most likely caused by complete occlusion of downstream intracranial arteries and commonly called as pseudothrombosis.

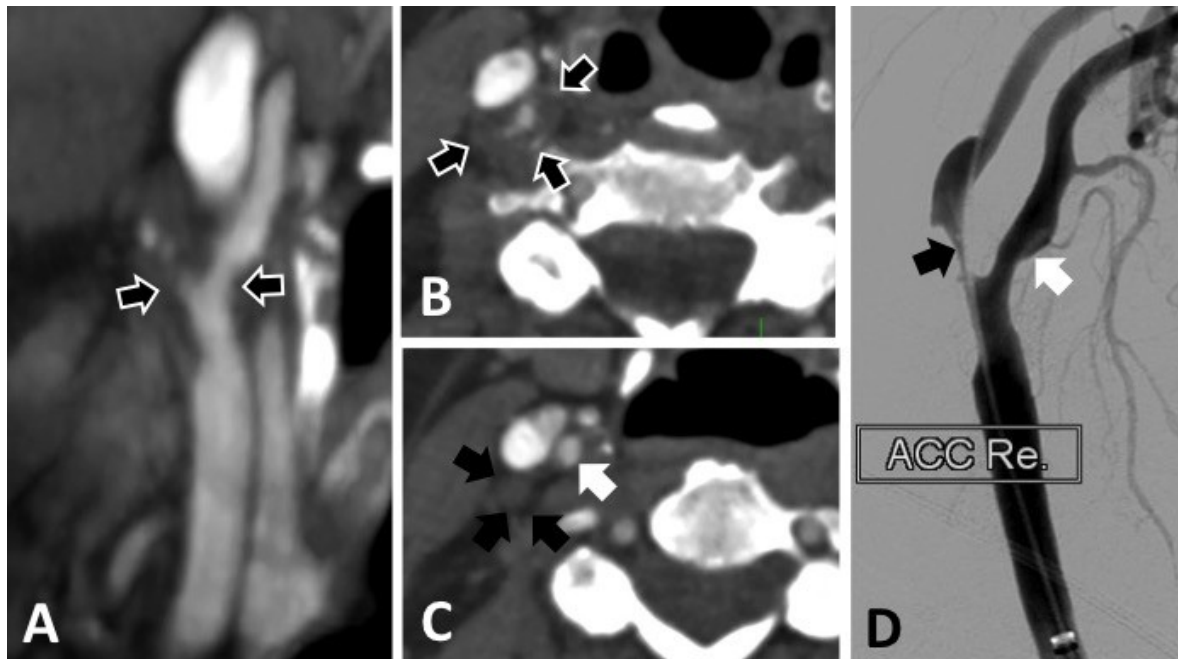


Figure 16 Pseud thrombosis

A 65 years old patient with right MCA occlusion (not shown). (A) Coronal section and (B) Axial section showing srCTA images with circumferential severe wall thickening of right carotid bifurcation (black arrows with white outline) causing high grade stenosis and minimal flow in the right ICA origin. (C) Axial section just downstream from the right ICA origin stenosis showed no contrast in right proximal ICA (black arrows) while right ECA (white arrow) remain opacified, suggestive of thrombosis of right ICA downstream to a high-grade stenosis at its origin. Nevertheless, when a right carotid DSA (D) injection was performed, contrast flowed through the near complete stenosis at right ICA origin (black arrow) and opacified the downstream ICA. This false negative thrombosis of right ICA on srCTA is called pseud thrombosis.

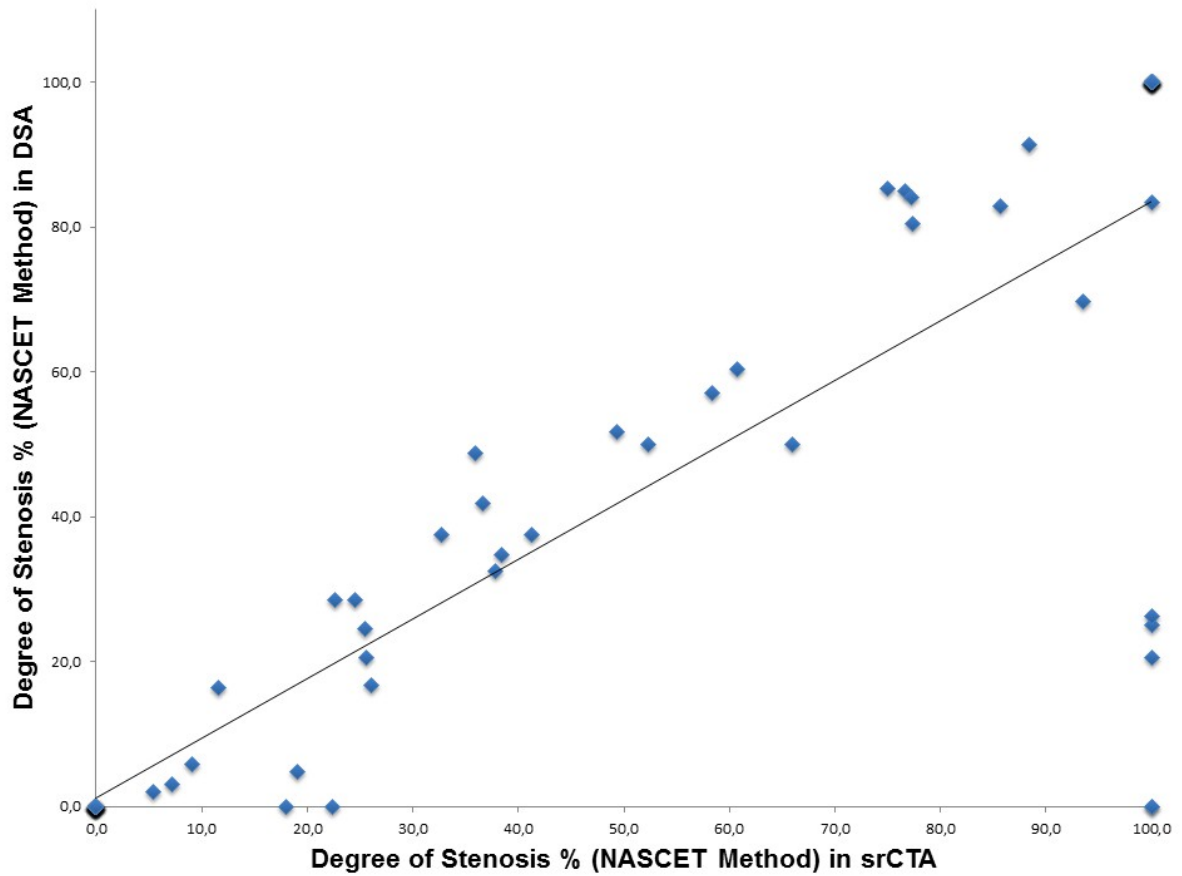


Figure 17 Scatterplot Chart for Degree of ICA stenosis in srCTA and DSA according to NASCET methods.

Overall, the percentage of proximal ICA stenosis on srCTA correlated well (see Figure 17) with DSA (Spearman's $\rho(77) = 0.87, p < 0.05$).

3.5 Artefacts

Number of Significant Artefacts Per Patient	Incidence	Percentage
0	111	77.6
1	19	13.3
2	7	4.9
3	6	4.2
4	0	0.0
5	0	0.0
6	0	0.0
Total	143	100.0

Table 4 Incidences of Number of Significant Artefacts Per Patient

22.4% of our patients have srCTA images which demonstrate at least one significant artefact which affects therapy planning (see Table 4). None of srCTA images have 4 or more significant artefacts affecting therapy planning.

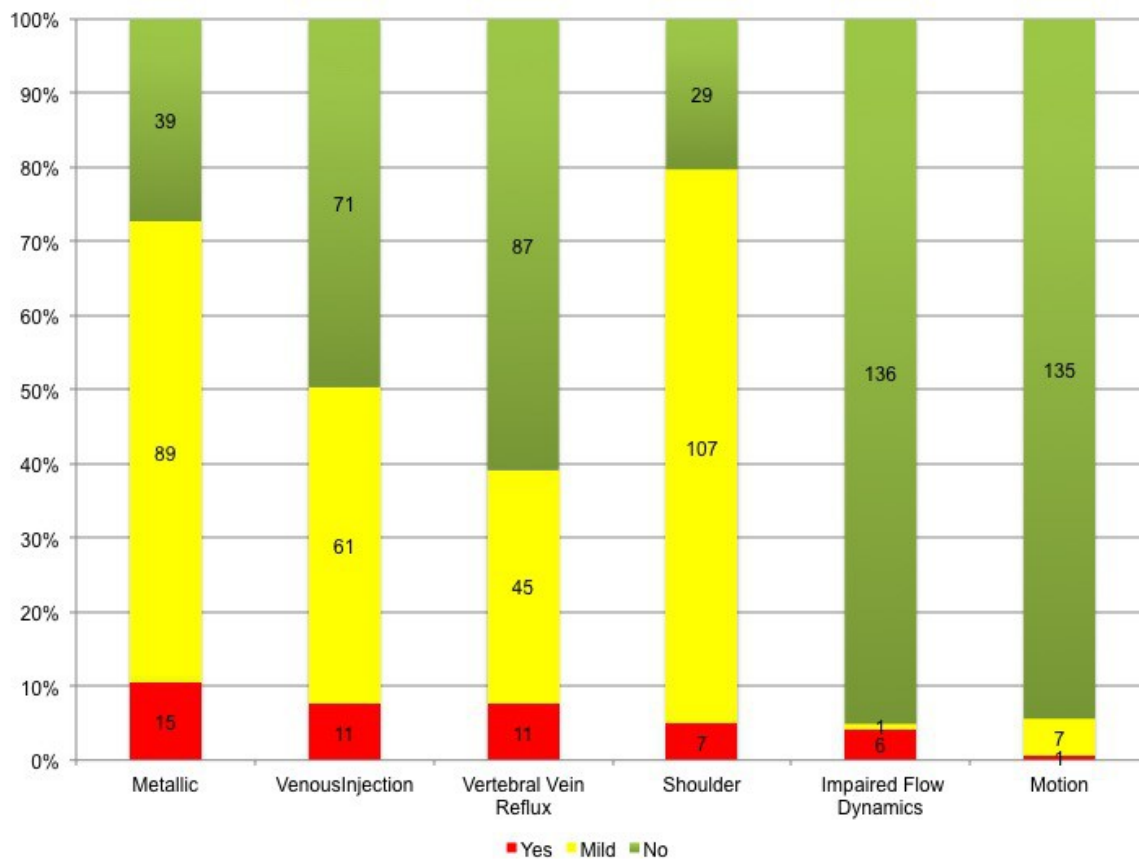


Figure 18 Incidence of artefacts

The highest percentage of artefact which severely obscured the srCTA image until affecting therapy planning was due to metallic hardware / dental fillings in 15 (10.5%) patients. In one patient with metallic prostheses in the cervical spine causing streak artefact, SEMAR reconstruction allowed visualisation of vertebral and carotid arteries (Figure 19). Photon starvation artefacts from the shoulder region were present in 114 (79.7%) patients, causing mild image obscuration in 107 (74.8%) of the patients and only severely affecting therapy planning in 7 (4.9%) patients. For a complete breakdown of the incidence of artefacts, please refer to Figure 18.

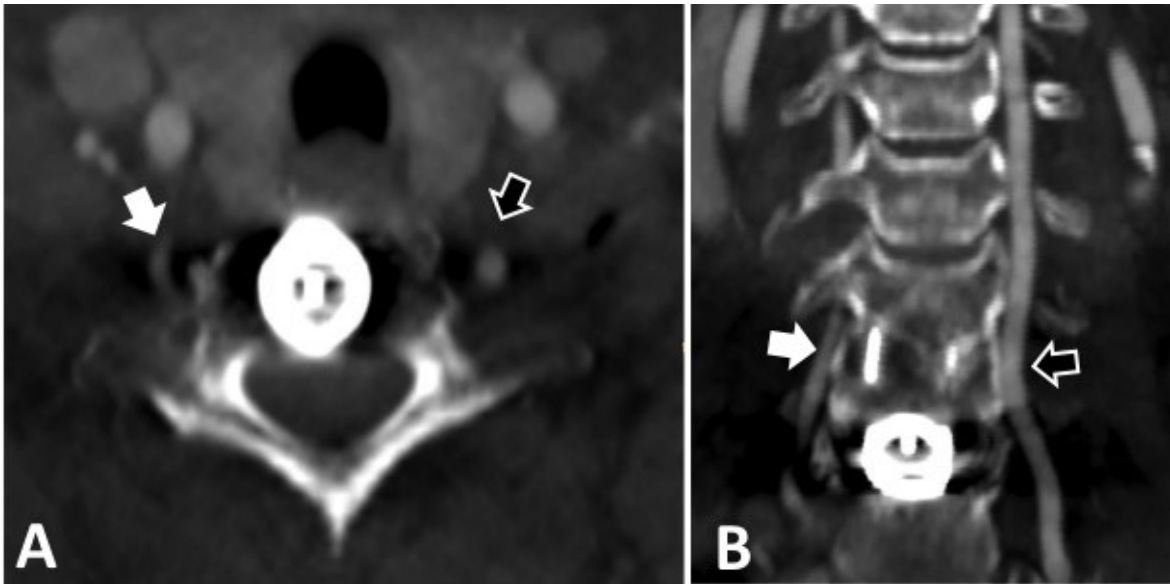


Figure 19 SEMAR.

Presence of dense vertebral prosthesis (HU up to 2995) in a 58 years old patient. CT Scanning with SEMAR activated. (A), Axial section and (B), Curved coronal reconstruction, showing presence of streak artefacts around the vertebral body prostheses. However, the right [(white arrow) partially shown due to U-loop] and left (black arrow) vertebral arteries were still visualised due to good opacifications within their lumens.

Flow related artefacts from venous injection and vertebral vein reflux severely obscured image quality, respectively in 11 (7.7%) patients. Reflux of contrast into IJV from venous injection were present in 7 patients (4.9%), the highest reflux was up to the level of middle ICA, 13 cm above the confluence of right IJV and right brachiocephalic vein. Motion artefact was present in 8 (5.6%) patients, causing mild blurring of arterial wall.

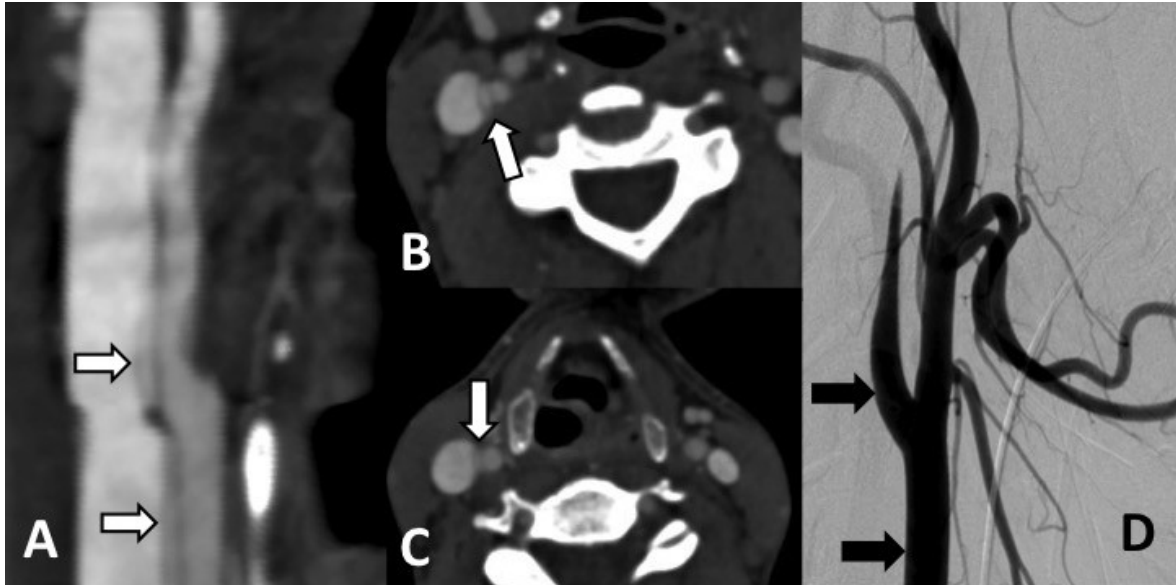


Figure 20 Pseudodissection.

A 28 years old patient presenting with right MCA thrombosis (not shown). Curved multiplanar reconstructed (A) and axial section images (B and C), showed an intraluminal linear filling defect (white arrows with black outline), resembling an intraluminal flap. However, DSA (D) of right ICA and right CCA showed no similar flap at the same area (black arrows). This artefact was in keeping with pseudodissection on srCTA. Note contrast stasis in the right ICA in DSA image (D) due to downstream right MCA thrombosis. The pseudodissection phenomenon in this instance could be due to interface misregistration between the carotid arteries and adjacent jugular veins.

In the artefacts due to impaired flow dynamics, 6 patients had false lesion artefacts, related to complete occlusion of the downstream ICA and high grade stenosis of proximal ICA, as described previously. The other patient had the appearance of intraluminal flap within the ICA, but was not proven on DSA (see Figure 20).

4 Discussion

4.1 Adequacy of scan range

In our patient cohort, the origins of all supra-aortic arteries were visualised in about 40% of the patients. In others the 16 cm scan range was inadequate. Nevertheless, the most important area, the carotid bifurcation, was always in the center of the scan range. Causes of stroke may be found in this region (stenosis, dissection or calcified plaques) which may need concurrent intracranial and extracranial endovascular treatments (20,21). The examination could probably be designed with the lower end of the scan range at the level of the aortic arch, accepting that in about 60 % of the patients the most superior segment of the skull will be not be included into the scan range. However, with that, the whole brain CTP would not be possible anymore. Another possibility would be to perform another second lower srCTA (22) with more mediastinal coverage, but this consumes more time, more radiation and may impair the perfusion scan. Although mediastinal pathology could be detected with such a scan protocol, the frequency of such findings is low (23).

4.2 Comparison to previous studies

Our srCTA neck acquisition is completely different compared to spiral-MS-CTA, which is the accepted gold standard technique for CTA. Siebert et al. (22) reported a series of 26 patients, where they performed extensive neuroimaging with a prototype 320-row detector CT scanner. srCTA neck was also performed, but as a separate modality. They reported that image quality of srCTA was inferior compared with spiral 64-slice CTA. They found geometric distortion phenomena especially at the borders of the shot and more pulsation artefacts compared to the 64-slice spiral CTA. However, their study was acquired with a prototype scanner and the results improved after hardware and software updates (24).

Our results differ from the results of Siebert et al. (22). We had the opportunity to work with the later generation 320-row detector volume CT and a different scanning protocol. In our study the srCTA of the cervical arteries was incorporated into the CTP protocol. We performed manual triggering of the srCTA upon early filling of the dural sinuses, thereby following a more individualized time attenuation curve. The benefits of manual triggering were two-fold: First, it compensated for difference in the cardiac output and second, potential shortening of examination time and radiation dose.

Our results compare favorably with the study of Kim et al. (19), whose study was performed on a 64-slice multidetector CT. Mean attenuation and percentage of arteries with HU \geq 150 were slightly better than reported by their study. This was despite lesser contrast volume (60 ml vs 70 ml) in our study, with CM being of equal 350 mg I/ml concentration. In contrast to Kim et al. (19), we found negative attenuation difference between the arteries and veins in our study, due to different timing of our srCTA scan. Notable also in both studies were the relatively higher contrast attenuation around carotid bifurcations, permitting better evaluation. Similar to objective assessment, visual assessment also showed good image quality of carotid bifurcations. We found that adequate intraluminal contrast allowed visualization of arteries even with vascular calcification.

4.3 Timing for Initiation of the Carotid Joggle

Timing of contrast arrival in the intended arteries was a very important factor influencing image quality. As srCTA neck was performed when contrast arrived in intracranial dural venous phase of CTP, this could potentially result in extracranial venous contamination. Dorn et al. [13] and Morhard et al. (25,26) saw more severe venous contamination when CTA was performed after CTP, and this was also the case in around 14% of our patients. However, as our srCTA image acquisition was performed at the start of venous phases of CTP and not completely thereafter, in almost all our patients, substantial contrast remained within the arteries, permitting adequate visualization. Therefore, in our opinion, manual triggering of srCTA acquisition achieved a

good balance between timing and image quality. Similar to bolus tracking or bolus timing, this triggering is operator dependent. Hence, the correct timing of this trigger should be performed by operators who are sufficiently trained to this protocol.

4.4 Correlation between srCTA and DSA

Our study showed there was a high qualitative and statistically significant quantitative correlation between DSA and srCTA of carotid bifurcations. In the six scenarios of discordance, catheter DSA at the carotid bifurcation proved to be superior to srCTA. Our findings are in agreement with recent studies(27–29), which shows absence of contrast flow in srCTA could be due to stasis downstream. A delayed imaging of the carotid bifurcation could be performed, but we concur with Wareham et al.(28), that this will be of limited value since a DSA will nonetheless be performed in the course of MTE and any delay could cost further brain damage. When a stenosis at the carotid bifurcation is detected on srCTA, catheter angiogram will be necessary before advancing into the ICA. Conversely, a normal carotid bifurcation on srCTA has high negative predictive value for a lesion in DSA and in the interest of time, a carotid DSA may be spared. However, due to the small size of this subgroup in our study, further research needs to be conducted before reaching this conclusion.

4.5 Artefacts affecting image quality

Image quality was affected by artefacts in our patients. However, the incidence of artefacts causing significant reduced image quality was generally lesser in our study compared to the previous 64 slice CT study (19). This was probably due to more delayed scan timing in our study, as well as application of iterative algorithm software reconstruction reducing image noise. The application of SEMAR also allows visualization of the arteries even with severe metallic streak artefacts, as long as adequate intravascular contrast was present. The low incidence of motion artefacts in our srCTA can be explained by the fast image acquisition with a single rotation at 0.5 sec.

5 Conclusion

With our current 320 detector large volume CT, joggle mode srCTA of neck incorporated into CTP was a feasible part of our stroke CT protocol, producing high image quality. The main drawback was incomplete coverage of supra-aortic arteries in two-thirds of patients. Timing of srCTA neck acquisition was an important element of the examination, the delay of which results in opacification of the extracranial venous segments.

6 References

1. Aho K, Harmsen P, Hatano S, Marquardsen J, Smirnov VE, Strasser T. Cerebrovascular disease in the community: results of a WHO collaborative study. *Bull World Health Organ.* 1980;58(1):113–30.
2. Katan M, Luft A. Global Burden of Stroke. *Semin Neurol.* 2018;38(2):208–11.
3. GBD 2016 Stroke Collaborators. Global, regional, and national burden of stroke, 1990-2016: a systematic analysis for the Global Burden of Disease Study 2016. *Lancet Neurol.* 2019 May;18(5):439–58.
4. Benjamin EJ, Muntner P, Alonso A, Bittencourt MS, Callaway CW, Carson AP, et al. Heart Disease and Stroke Statistics-2019 Update: A Report From the American Heart Association. *Circulation.* 2019 05;139(10):e56–528.
5. Engelhardt E. Apoplexy, cerebrovascular disease, and stroke: Historical evolution of terms and definitions. *Dement neuropsychol.* 2017 Dec;11(4):449–53.
6. Friedman SG. The first carotid endarterectomy. *J Vasc Surg.* 2014 Dec;60(6):1703-1708.e1-4.
7. Canadian Cooperative Study Group. A randomized trial of aspirin and sulfipyrazone in threatened stroke. *N Engl J Med.* 1978 13;299(2):53–9.
8. Zivin JA. Acute stroke therapy with tissue plasminogen activator (tPA) since it was approved by the U.S. Food and Drug Administration (FDA). *Ann Neurol.* 2009 Jul;66(1):6–10.
9. Wahlgren N, Moreira T, Michel P, Steiner T, Jansen O, Cognard C, et al. Mechanical thrombectomy in acute ischemic stroke: Consensus statement by ESO-Karolinska Stroke Update 2014/2015, supported by ESO, ESMINT, ESNR and EAN. *Int J Stroke.* 2016 Jan;11(1):134–47.
10. Saver JL. Time is brain--quantified. *Stroke.* 2006 Jan;37(1):263–6.

11. Gomez CR. Editorial: Time is brain! *J Stroke Cerebrovasc Dis*. 1993;3(1):1–2.
12. Ledezma CJ, Wintermark M. Multimodal CT in stroke imaging: new concepts. *Radiol Clin North Am*. 2009 Jan;47(1):109–16.
13. Garg N, Eshkar N, Tanenbaum L, Cohen B, Sen S. Computed tomography angiographic correlates of early computed tomography signs in acute ischemic stroke. *J Neuroimaging*. 2004 Jul;14(3):242–5.
14. González RG, Copen WA, Schaefer PW, Lev MH, Pomerantz SR, Rapalino O, et al. The Massachusetts General Hospital acute stroke imaging algorithm: an experience and evidence based approach. *J Neurointerv Surg*. 2013 May;5 Suppl 1:i7-12.
15. Ezzeddine MA, Lev MH, McDonald CT, Rordorf G, Oliveira-Filho J, Aksoy FG, et al. CT angiography with whole brain perfused blood volume imaging: added clinical value in the assessment of acute stroke. *Stroke*. 2002 Apr;33(4):959–66.
16. Scaroni R, Tambasco N, Cardaioli G, Parnetti L, Paloni F, Boranga B, et al. Multimodal use of computed tomography in early acute stroke, part 2. *Clin Exp Hypertens*. 2006 May;28(3–4):427–31.
17. Zhu G, Michel P, Aghaebrahim A, Patrie JT, Xin W, Eskandari A, et al. Computed tomography workup of patients suspected of acute ischemic stroke: perfusion computed tomography adds value compared with clinical evaluation, noncontrast computed tomography, and computed tomography angiogram in terms of predicting outcome. *Stroke*. 2013 Apr;44(4):1049–55.
18. de Lucas EM, Sánchez E, Gutiérrez A, Mandly AG, Ruiz E, Flórez AF, et al. CT protocol for acute stroke: tips and tricks for general radiologists. *Radiographics*. 2008 Oct;28(6):1673–87.
19. Kim JJ, Dillon WP, Glastonbury CM, Provenzale JM, Wintermark M. Sixty-four-section multidetector CT angiography of carotid arteries: a systematic analysis of image quality and artifacts. *AJNR Am J Neuroradiol*. 2010 Jan;31(1):91–9.

20. Steglich-Arnholm H, Holtmannspötter M, Kondziella D, Wagner A, Stavngaard T, Cronqvist ME, et al. Thrombectomy assisted by carotid stenting in acute ischemic stroke management: benefits and harms. *J Neurol*. 2015 Dec;262(12):2668–75.
21. Cohen JE, Gomori M, Rajz G, Moscovici S, Leker RR, Rosenberg S, et al. Emergent stent-assisted angioplasty of extracranial internal carotid artery and intracranial stent-based thrombectomy in acute tandem occlusive disease: technical considerations. *J Neurointerv Surg*. 2013 Sep 1;5(5):440–6.
22. Siebert E, Bohner G, Dewey M, Masuhr F, Hoffmann KT, Mews J, et al. 320-slice CT neuroimaging: initial clinical experience and image quality evaluation. *Br J Radiol*. 2009 Jul;82(979):561–70.
23. Deipolyi AR, Hamberg LM, González RG, Hirsch JA, Hunter GJ. Diagnostic yield of emergency department arch-to-vertex CT angiography in patients with suspected acute stroke. *AJNR Am J Neuroradiol*. 2015 Feb;36(2):265–8.
24. Siebert E, Bohner G, Dewey M, Hoffmann KT, Mews J, Engelken F, et al. Letter to the editor concerning “320-slice CT neuroimaging: initial clinical experience and image quality evaluation” (Siebert E et al: *Br J Radiol* 2009;82:561-70). *Br J Radiol*. 2009 Jul;82(979):615.
25. Dorn F, Liebig T, Muenzel D, Meier R, Poppert H, Rummeny EJ, et al. Order of CT stroke protocol (CTA before or after CTP): impact on image quality. *Neuroradiology*. 2012 Feb;54(2):105–12.
26. Morhard D, Wirth CD, Reiser MF, Schulte-Altendorneburg G, Ertl-Wagner B. Optimal sequence timing of CT angiography and perfusion CT in patients with stroke. *Eur J Radiol*. 2013 Jun;82(6):e286-289.
27. Marquering HA, Nederkoorn PJ, Beenen LF, Lycklama à Nijeholt GJ, van den Berg R, Roos YB, et al. Carotid pseudo-occlusion on CTA in patients with acute ischemic stroke: a concerning observation. *Clin Neurol Neurosurg*. 2013 Sep;115(9):1591–4.

28. Wareham J, Crossley R, Barr S, Mortimer A. Cervical ICA pseudo-occlusion on single phase CTA in patients with acute terminal ICA occlusion: what is the mechanism and can delayed CTA aid diagnosis? *J Neurointerv Surg.* 2018 Oct;10(10):983–7.
29. Akpınar S, Gelener P, Yilmaz G. Aetiologies of internal carotid artery pseudo-occlusions in acute stroke patients: what neurointerventionalists can expect. *BJR.* 2017 Feb;90(1070):20160352.